

October, 1995

Equation of State of an Interacting Pion Gas with Realistic $\pi-\pi$ Interactions

R. Rapp and J. Wambach¹

*Institut für Kernphysik (Theorie)
Forschungszentrum Jülich
D-52425 Jülich
Germany*

Abstract

Within the finite-temperature Greens-function formalism we study the equation of state of a hot interacting pion gas at zero chemical potential. Employing realistic $\pi\pi$ meson-exchange interactions we selfconsistently calculate the in-medium single-pion selfenergy and the $\pi\pi$ scattering amplitude in the quasiparticle approximation. These quantities are then used to evaluate the thermodynamic potential, $\Omega_\pi(T)$, from which the state variables: pressure-, entropy- and energy-density can be derived. In contrast to earlier calculations based on the low-energy Weinberg Lagrangian we find an overall increase as compared to the free-gas results. We also consider the possibility of a dropping ρ -meson mass as suggested by the 'Brown-Rho Scaling' law.

PACS Indices: 13.75.Lb
24.10.Cn
25.75.+rq

¹also at: Department of Physics, University of Illinois at Urbana-Champaign, 1110 West Green St., Urbana, IL 61801-3080, USA

1 Introduction

In recent years much effort has been put into the study of ultrarelativistic heavy-ion collisions (URHIC's). The main objective of these experiments is to create a new state of hadronic matter, the Quark–Gluon plasma (QGP). However, it is not settled if the current generation of experiments at the BNL–AGS and CERN–SpS is able to generate sufficiently high energy densities to make the transition. On the other hand, lattice gauge calculations, although not yet at the stage of making accurate predictions, suggest the occurrence of a different kind of phase transition associated with the restoration of chiral symmetry. This 'chiral phase transition' is expected to occur prior to the deconfinement transition at a critical temperature of $T_c^\chi = 140 - 170$ MeV. Precursors of chiral symmetry restoration may well establish before that, e.g. the dropping of vector meson masses as proposed by Brown and Rho [1, 2] based on chiral effective Lagrangians and further corroborated by Hatsuda et al. [3] within the QCD sum rule approach.

In central collisions at the AGS, the midrapidity region is characterized by highly compressed nuclear matter due to an almost entire stopping of the Lorentz–contracted colliding nuclei. Even at SpS energies, where the stopping power is much less, one encounters sizable baryon densities at central rapidity, leading to an appreciable impact on the in–medium properties of the produced secondaries (mostly pions). At the Brookhaven Relativistic Heavy Ion Collider (RHIC), on the other hand, baryon densities in the central zone are expected to be very small, such that, after hadronization, this zone will be populated by a dense pion gas.

Many aspects of a hot, interacting pion gas have been studied in the literature so far, e.g. single–pion 'optical' potentials [4, 5, 6, 7], mean free paths [8], in–medium $\pi\pi$ cross sections [9, 10, 6], the equation of state [11, 12], hydrodynamic properties [13, 14] as well as numerical solutions of a bosonic Boltzmann equation [15] simulating the dynamics of URHIC's prior to freeze out.

In this article we want to concentrate on the equilibrium properties of a thermal pion gas, *i.e.* the equation of state (EOS). Within the relativistic virial expansion, restricted to

two–body collisions, Welke et al. [11] have previously employed an empirical parametrization of the experimental vacuum $\pi\pi$ scattering phase shifts in s– and p–wave as their basic input for calculating the number–, energy–, pressure– and entropy–densities of an interacting gas of pions. They have found that the net effect of the $\pi\pi$ interaction stems from the resonant $J1=11-(\rho-)$ channel leading to an increase of the thermodynamic state variables, relative to the free gas, for temperatures $T \gtrsim 100$ MeV. Quantitatively this contribution is comparable to what one would expect from an admixture of free ρ mesons. In other words, the rather sharp ρ resonance in the $\pi\pi$ interaction resembles the contribution from free ρ mesons, a mechanism well–known from the Beth–Uhlenbeck formalism [16]. Bunatian and Kämpfer [12] have pursued a rather different approach, based on finite temperature Green’s functions in the imaginary time formalism. As the $\pi\pi$ interaction they employed the Weinberg Lagrangian [17], known to account for low–energy s–wave $\pi\pi$ scattering. As a result of their selfconsistent calculations in the Hartree approximation the thermodynamic state variables exhibit a *decrease* for temperatures $T \gtrsim 150$ MeV.

The aim of the present paper is to recalculate the EOS by both employing a realistic $\pi\pi$ model capable of describing the vacuum scattering data up to rather high energies and by taking into account the in–medium modifications of single–pions as well as of the $\pi\pi$ scattering amplitude selfconsistently and to all orders. Our formalism for calculating the thermodynamics will be the one used by Bunatian and Kämpfer, but extended beyond the Hartree approximation. The $\pi\pi$ interaction we use is the meson–exchange model developed by the Jülich group [18] which, on a microscopic level, describes the $\pi\pi$ scattering data in the various partial waves up to CMS energies of 1.5 GeV.

Our article is organized as follows: in sect. 2 we present the formalism for calculating the thermodynamic potential $\Omega_\pi(T)$. In sect. 3 we derive from it the thermodynamic state variables, *i.e.* the pressure–, entropy– and energy–density, and discuss the numerical results within the Jülich $\pi\pi$ model with no in–medium modifications applied to the meson–exchange potentials (Brueckner theory). In sect. 4 we consider the possibility of additional medium effects on the exchanged mesons in terms of a dropping ρ –meson mass. In sect. 5

we summarize and make some concluding remarks.

2 The Thermodynamic Potential of Interacting Pions

The starting point of our analysis is the well-known expression for the thermodynamic potential of a gas of interacting bosons at finite temperature [19]. In case of interacting pions it reads

$$\Omega_\pi(T) = \Omega_\pi^Q(T) + \Omega_{\pi\pi}(T) \quad (1)$$

where the first term represents the quasiparticle contribution while the second term arises from interactions between the quasiparticles. For thermodynamic consistency both terms have to be considered.

In terms of the single-pion propagator

$$D_\pi(\omega_+, k) = \left(\omega_+^2 - m_\pi^2 - k^2 - \Sigma_\pi(\omega_+, k) \right)^{-1}, \quad (2)$$

($\omega_+ \equiv \omega + i\eta$), where $\Sigma_\pi(\omega_+, k)$ denotes the pion selfenergy, the quasiparticle contribution is given by

$$\Omega_\pi^Q(T) = -\frac{3}{2} \int \frac{d^3 k}{(2\pi)^3} \int \frac{d\omega}{\pi} f^\pi(\omega) \operatorname{Im}\{\ln[-D_\pi^{-1}(\omega_+, k)] - D_\pi(\omega_+, k)\Sigma_\pi(\omega_+, k)\} \quad (3)$$

where $f^\pi(\omega) = (\exp(\omega/T) - 1)^{-1}$ is the thermal Bose factor. The interaction contribution, $\Omega_{\pi\pi}(T)$, is the sum of all 'skeleton diagrams' arising from a perturbative expansion of the scattering amplitude. Within the Matsubara formalism the contribution from n -th order meson exchange can be written as

$$\Omega_{\pi\pi}^{(n)}(T) = \frac{3}{2} \frac{1}{4n} (-T) \int \frac{d^3 k}{(2\pi)^3} \sum_{z_\nu} D_\pi(z_\nu, k) \Sigma_\pi^{(n)}(z_\nu, k). \quad (4)$$

This can be pictured as closing the two external legs of the pion selfenergy. The factor $1/4n$ corrects for overcounting [19] induced by the possible ways of regenerating the n -th order pion selfenergy by cutting a single-pion line in the diagrams of $\Omega_{\pi\pi}(T)$. For the case

of $\pi\pi$ contact interactions as where considered in refs. [12, 20] the appropriate counting factor is $1/2n$ due to the absence of u-channel exchange graphs.

Let us first turn to the calculation of the two-body interaction contribution $\Omega_{\pi\pi}(T)$.

2.1 Lowest-Order Contributions to $\Omega_{\pi\pi}(T)$

To lowest order ($n = 1$) $\Omega_{\pi\pi}(T)$ has already been calculated in ref. [12]. In the context of a $\pi\pi$ meson-exchange potential it reads

$$\Omega_{\pi\pi}^{(1)}(T) = \frac{3}{8} \int \frac{d^3k}{(2\pi)^3} \int \frac{d^3p}{(2\pi)^3} \int \frac{d\omega}{\pi} f^\pi(\omega) \text{Im}D_\pi(\omega, k) \times \int \frac{d\omega'}{\pi} f^\pi(\omega') \text{Im}D_\pi(\omega', p) M_{\pi\pi}^{(1)}(\omega + \omega', k, p) , \quad (5)$$

where $M_{\pi\pi}^{(1)}$ denotes the spin-isospin averaged, first-order forward scattering amplitude. Employing the quasiparticle approximation (QPA) for the single-pion propagator,

$$\text{Im}D_\pi(\omega, k) = -\frac{\pi}{2e_k} [\delta(\omega - e_k) - \delta(\omega + e_k)] , \quad (6)$$

eq. (5) can be simplified as

$$\begin{aligned} \Omega_{\pi\pi}^{(1)}(T) = & \frac{3}{8} \int \frac{k^2 dk}{2\pi^2} \int \frac{p^2 dp}{(2\pi)^2} \int_{+1}^{-1} dx \frac{1}{2e_k} \frac{1}{2e_p} \times \\ & \{ M_{\pi\pi}^{(1)}(e_p + e_k, \vec{k}, \vec{p}) [f^\pi(e_k) f^\pi(e_p) + (f^\pi(e_k) + 1)(f^\pi(e_p) + 1)] \\ & + M_{\pi\pi}^{(1)}(e_k - e_p, \vec{k}, \vec{p}) [f^\pi(e_k)(f^\pi(e_p) + 1) + (f^\pi(e_k) + 1)f^\pi(e_p)] \} , \end{aligned} \quad (7)$$

where $x \equiv \cos \Theta$, $\Theta = \angle(\vec{k}, \vec{p})$. The quasiparticle energies e_k are determined from the selfconsistent solution of the Dyson equation:

$$e_k^2 = m_\pi^2 + k^2 + \text{Re}\Sigma_\pi(e_k, k) . \quad (8)$$

The right-hand side (*rhs*) of eq. (7) diverges due to the various '1's appearing in the occupation factors. However, when the thermodynamic potential is defined relative to the physical vacuum by only considering the difference between the values at $T = 0$ and finite T then it remains finite. This is achieved by removing the '1's in eq. (7) [12]. Thus

$$\begin{aligned}
\tilde{\Omega}_{\pi\pi}^{(1)}(T) &\equiv \Omega_{\pi\pi}^{(1)}(T) - \Omega_{\pi\pi}^{(1)}(0) \\
&\approx \frac{3}{8} \int \frac{k^2 dk}{2\pi^2 2e_k} \int \frac{p^2 dp}{(2\pi)^2 2e_p} 2f^\pi(e_k)f^\pi(e_p) \times \\
&\quad \int_{+1}^{-1} dx \{ M_{\pi\pi}^{(1)}(e_p + e_k, \vec{k}, \vec{p}) + M_{\pi\pi}^{(1)}(e_k - e_p, \vec{k}, \vec{p}) \} . \tag{9}
\end{aligned}$$

In the following we shall suppress the tilde and always refer to subtracted quantities. For practical evaluations, the M -amplitude has to be transformed into the CMS of the two scattered pions, thereby neglecting the medium dependence of $M_{\pi\pi}$ on the total momentum $\vec{P} = \vec{k} + \vec{p}$ of the pion pair. Then the total CMS energy is identified as

$$E^2 \equiv s = (e_k \pm e_p)^2 - (\vec{k} + \vec{p})^2 \tag{10}$$

and, by requiring Lorentz invariance, the relative CMS momentum of the pions is obtained as

$$(\vec{q})^2 = \frac{1}{s} \left[\frac{1}{4} (s - (e_k^2 - k^2) - (e_p^2 - p^2))^2 - (e_k^2 - k^2)(e_p^2 - p^2) \right] . \tag{11}$$

Using $ds = -2pkdx$ we can rewrite eq. (9) as

$$\Omega_{\pi\pi}^{(1)}(T) = \frac{3}{8} \int \frac{k^2 dk}{(2\pi)^2 2e_k} \int \frac{p^2 dp}{(2\pi)^2 2e_p} f^\pi(e_k) f^\pi(e_p) [I_A^{(1)} + I_B^{(1)}] \tag{12}$$

with

$$\begin{aligned}
I_{A/B}^{(1)} &\equiv \int_{E_{min}^{A/B}}^{E_{max}^{A/B}} E dE M_{\pi\pi}^{(1)}(E, q, q) , \\
E_{max}^{A/B} &= (e_k \pm e_p)^2 - k^2 - p^2 + 2kp , \\
E_{min}^{A/B} &= (e_k \pm e_p)^2 - k^2 - p^2 - 2kp , \tag{13}
\end{aligned}$$

which is the main result of this subsection.

2.2 Higher-Order Contributions to $\Omega_{\pi\pi}(T)$

Within the meson-exchange framework, the full $M_{\pi\pi}$ -amplitude is obtained by solving a Lippmann–Schwinger type equation (LSE), which, in our case [18], results from the

Blankenbecler–Sugar reduction [21] of the covariant Bethe–Salpeter equation. In a given partial–wave/isospin channel JI the scattering equation reads

$$M_{\pi\pi}^{JI}(E, q_1, q_2) = V_{\pi\pi}^{JI}(E, q_1, q_2) + \int_0^\infty \frac{dq}{(2\pi)^2} q^2 V_{\pi\pi}^{JI}(E, q_1, q) G_{\pi\pi}(E, q) M_{\pi\pi}^{JI}(E, q, q_2) , \quad (14)$$

where $G_{\pi\pi}(E, q)$ denotes the two–pion propagator of the intermediate state and $V_{\pi\pi} \equiv M_{\pi\pi}^{(1)}$ are the Born amplitudes (pseudopotentials) derived from an effective meson Lagrangian. Schematically, the scattering equation (14) can also be written as a perturbative expansion

$$\begin{aligned} M &= V + VGM \\ &= V + VGV + VGVGV + \dots \\ &\equiv M^{(1)} + M^{(2)} + M^{(3)} + \dots . \end{aligned} \quad (15)$$

Beyond the Born approximation, *i.e.* for $n \geq 2$, the M –amplitude acquires an imaginary part due to the intermediate two–pion states being on–shell. Consequently, $\Sigma_\pi^{(n)}$ also becomes a complex quantity. In order to evaluate eq. (4) for $n \geq 2$, we therefore employ the standard procedure of inserting the spectral representations of the single–pion propagator and the selfenergy:

$$\begin{aligned} D_\pi(z_\nu, k) &= - \int \frac{d\omega'}{\pi} \frac{Im D_\pi(\omega', k)}{z_\nu - \omega' + i\eta} \\ \Sigma_\pi^{(n)}(z_\nu, k) &= - \int \frac{d\omega}{\pi} \frac{Im \Sigma_\pi^{(n)}(\omega, k)}{z_\nu - \omega + i\eta} - Re \Sigma_\pi^{(n)}(0, k) \\ &= - \int \frac{d\omega}{\pi} Im \Sigma_\pi^{(n)}(\omega, k) \left(\frac{1}{z_\nu - \omega + i\eta} + \frac{\mathcal{P}}{\omega} \right) . \end{aligned} \quad (16)$$

According to the findings in ref. [22] the dispersion relation for the pion selfenergy has to be supplemented with a subtraction at zero energy.

The Matsubara sum in eq. (4) can now be performed analytically. The imaginary part of the pion selfenergy has been derived in ref. [22] and we can immediately generalize the

result to the n -th order contribution:

$$Im\Sigma_\pi^{(n)}(\omega_+, k) = - \int \frac{d^3 p}{(2\pi)^3} \int \frac{d\omega'}{\pi} ImM_{\pi\pi}^{(n)}(\omega_+ + \omega', \vec{k}, \vec{p}) ImD_\pi(\omega'_+, p) [f^\pi(\omega') - f^\pi(\omega + \omega')] . \quad (17)$$

Injecting eqs. (16), (17) into eq. (4) results in the following, exact expression for the n -th order scattering contribution to the thermodynamic potential:

$$\Omega_{\pi\pi}^{(n)}(T) = -\frac{3}{2} \frac{1}{4n} \int \frac{d^3 k}{(2\pi)^3} \int \frac{d^3 p}{(2\pi)^3} \int \frac{dE'}{\pi} \int \frac{d\omega}{\pi} \int \frac{d\omega'}{\pi} ImD_\pi(\omega', p) ImD_\pi(\omega, k) \times \\ ImM_{\pi\pi}^{(n)}(E', \vec{k}, \vec{p}) \left\{ \frac{[f^\pi(\omega') - f^\pi(E')] [\omega f^\pi(\omega) - (E' - \omega') f^\pi(E' - \omega')]}{(\omega_+ + \omega' - E')(E' - \omega')} \right\} . \quad (18)$$

Note that the imaginary part of the *rhs*, given by the δ -function part of $1/(\omega_+ + \omega' - E')$, vanishes due to the simultaneous disappearance of the second occupation factor – as it should, since $\Omega_{\pi\pi}(T)$ is a real quantity. Applying the QPA, eq. (6), and performing the trivial angular integrations leads to

$$\Omega_{\pi\pi}^{(n)}(T) = -\frac{3}{2} \frac{1}{4n} \int \frac{k^2 dk}{2\pi^2 2e_k} \int \frac{p^2 dp}{(2\pi)^2 2e_p} \int_0^1 dx \int_0^\infty \frac{dE'}{\pi} ImM_{\pi\pi}^{(n)}(E', q, q) \times \\ 2[F^\pi(E', k, p) + G^\pi(E', k, p)] , \quad (19)$$

where

$$F^\pi(E', k, p) = \frac{[f^\pi(e_p) - f^\pi(E')] [e_k f^\pi(e_k) - (E' - e_p) f^\pi(E' - e_p)]}{(e_k + e_p - E')(E' - e_p)} \\ + \frac{[f^\pi(e_p) + f^\pi(E')] [e_k f^\pi(e_k) - (E' + e_p) f^\pi(E' + e_p)]}{(e_k + e_p + E')(E' + e_p)} \\ G^\pi(E', k, p) = -\frac{[f^\pi(e_p) - f^\pi(E')] [e_k f^\pi(e_k) - (E' - e_p) f^\pi(E' - e_p)]}{(-e_k + e_p - E')(E' - e_p)} \\ + \frac{[f^\pi(e_p) + f^\pi(E')] [e_k f^\pi(e_k) - (E' + e_p) f^\pi(E' + e_p)]}{(e_k - e_p - E')(E' + e_p)} . \quad (20)$$

The second term in F^π arises from the negative-energy part of the E' -integration. It is obtained from the first term when replacing $E' \rightarrow (-E')$ and introducing an overall minus sign due to the symmetry $ImM_{\pi\pi}(-E' + i\eta) = -ImM_{\pi\pi}(E' + i\eta)$. Similarly, the function G^π is generated from F^π when replacing $e_k \rightarrow (-e_k)$ with an overall minus sign due

to the antisymmetry of the single-pion spectral function, eq. (6). Since the 4-momenta $(\omega, \vec{k}), (\omega', \vec{p})$ enter eq. (18) on equal footing we obtain an additional factor of 2 for the negative energy contributions of $Im D_\pi(\omega', p)$.

It is not to be expected that, evaluating $\Omega_{\pi\pi}^{(n)}(T)$ order by order, leads to a convergent series. For the LSE (15) the Born series does not converge and, although there appears an additional factor $1/n$ when summing the thermodynamic potential

$$\Omega_{\pi\pi}(T) = \sum_{n=1}^{\infty} \Omega_{\pi\pi}^{(n)}(T) , \quad (21)$$

it may not change the convergence behavior of the series. In particular, the s-channel pole graphs (i.e. genuine $\pi\pi$ -resonances) turn out to be problematic, since they exhibit non-integrable singularities in each order $n \geq 2$. In the following we will discuss them in more detail.

2.2.1 s–Channel Pole graphs

In the Jülich model of Lohse et al. [18] a genuine resonance is characterized by a separable Born term of the form

$$V_\alpha^{JI}(E', q_1, q_2) = v_{\pi\pi\alpha}(q_1) D_\alpha^0(E') v_{\pi\pi\alpha}(q_2) \quad (22)$$

with the bare resonance propagator

$$D_\alpha^0(E') = \frac{1}{E'^2 - (m_\alpha^{(0)})^2} , \quad (23)$$

$m_\alpha^{(0)}$ being the bare mass of the resonance α with spin–isospin JI . The vertex functions contain coupling constants, isospin and form factors as well as kinematic factors specific to the spin–momentum part of the coupling.

As is well known, the LSE can be solved analytically for the case of a separable potential [23] which yields

$$\begin{aligned} M_\alpha^{JI}(E', q_1, q_2) &= v_{\pi\pi\alpha}(q_1) D_\alpha^0(E') v_{\pi\pi\alpha}(q_2) \sum_{n=1}^{\infty} \left[\frac{I_\alpha(E')}{E'^2 - (m_\alpha^{(0)})^2} \right]^{n-1} \\ &= \frac{v_{\pi\pi\alpha}(q_1) v_{\pi\pi\alpha}(q_2)}{E'^2 - (m_\alpha^{(0)})^2 - I_\alpha(E')} , \end{aligned} \quad (24)$$

where

$$I_\alpha(E') = \int q^2 dq v_{\pi\pi\alpha}(q)^2 G_{2\pi}(E', q) \quad (25)$$

is just the intermediate $\pi\pi$ bubble. In eq. (24) the summation index is chosen such that $n = 1$ corresponds to the lowest-order (Born) term. Apparently the n -th order contribution in eq. (24) exhibits a pole of order n at $E' = m_\alpha^{(0)}$, leading to divergencies in the E' -integration of eq. (19). The infinite sum of $\pi\pi$ bubbles, on the other hand, simply renormalizes the bare propagator generating a mass shift and a finite width, given by $ReI_\alpha(E')$ and $ImI_\alpha(E')$, respectively. As we shall show now, this implies the possibility of summing the $\Omega_{\pi\pi\alpha}^{(n)}(T)$ contributions to all orders, thereby avoiding any divergencies.

The evaluation of eq. (21) for pure resonance scattering involves the following sum:

$$\begin{aligned} \Omega_{\pi\pi\alpha}(T) &\propto \sum_{n=2}^{\infty} \frac{1}{n} Im M_{\pi\pi\alpha}^{(n)}(E', q, q) \\ &= v_{\pi\pi\alpha}(q)^2 D_\alpha^0(E') Im \left[\sum_{n=2}^{\infty} \frac{1}{n} \left(\frac{I_\alpha(E')}{E'^2 - (m_\alpha^{(0)})^2} \right)^n \right] \\ &= v_{\pi\pi\alpha}(q)^2 Im \left[\frac{1}{I_\alpha(E')} \sum_{n=1}^{\infty} \frac{1}{n} \left(\frac{I_\alpha(E')}{E'^2 - (m_\alpha^{(0)})^2} \right)^n \right], \end{aligned} \quad (26)$$

where we have added a zero in form of the ($n = 1$)-term (Born term), which does not generate any imaginary part. Using the identity

$$\ln(1 - x) = - \sum_{n=1}^{\infty} \frac{x^n}{n}, \quad (27)$$

we are now able to perform the infinite sum in eq. (26). The resulting thermodynamic potential reads

$$\begin{aligned} \Omega_{\pi\pi\alpha}(T) &= -\frac{3}{8} \int \frac{k^2 dk}{2\pi^2 2e_k} \int \frac{p^2 dp}{(2\pi)^2 2e_p} \int_{+1}^{-1} dx \int_0^{\infty} \frac{dE'}{\pi} SI(\alpha) v_{\pi\pi\alpha}(q)^2 \times \\ &\quad Im \left\{ \frac{(-1)}{I_\alpha(E')} \ln \left[1 - \frac{I_\alpha(E')}{E'^2 - (m_\alpha^{(0)})^2} \right] \right\} 2 [F^\pi(E', k, p) + G^\pi(E', k, p)], \end{aligned} \quad (28)$$

with

$$SI(\alpha) = \frac{(2J+1)(2I+1)}{3} \quad (29)$$

being the spin-isospin weighting factor of the corresponding $\pi\pi$ resonance channel. When numerically evaluating eq. (28) in the Jülich Model, one obtains results far too large to be realistic. A closer inspection shows that, for fixed momentum k , the p -integration dominantly picks up high-momentum components. The reason for that can be traced back to the weak suppression in the (dipole) form factors entering the vertex functions $v_{\pi\pi\alpha}(q)$,

$$F(q) = \left(\frac{2\Lambda_\alpha^2 + m_\alpha^2}{2\Lambda_\alpha^2 + 4\omega_q^2} \right)^2. \quad (30)$$

In the limit of large p -values, $p \gg k$, the CMS momentum q behaves like $q^2 \propto p$, i.e. one essentially loses four powers of momentum in $v_{\pi\pi\alpha}(q)^2 \propto F(q)^2$. Note that the occupation factors F^π and G^π , eq. (20), contain terms independent of $f^\pi(e_p)$ such that no 'thermal' suppression is at work. To overcome this unrealistic behavior we have decided to replace the form factor at each vertex by

$$F(q) \rightarrow \sqrt{F(k)F(p)} = \left(\frac{2\Lambda_\alpha^2 + m_\alpha^2}{2\Lambda_\alpha^2 + 4\omega_k^2} \right) \left(\frac{2\Lambda_\alpha^2 + m_\alpha^2}{2\Lambda_\alpha^2 + 4\omega_p^2} \right), \quad (31)$$

which restricts the relevant momentum ranges in eq. (28) to a realistic domain of $p, k \lesssim \Lambda_\alpha$ (e.g. $\Lambda_\rho = 3.3$ GeV in the Jülich model).

2.2.2 t-Channel Vector-Meson Exchange

In the Jülich model the dominant contribution to the low-energy $\pi\pi$ interaction is generated by t-channel exchange of the ρ meson. The corresponding Born amplitude is of the non-separable form

$$V_{\rho ex}^{JI}(E', q_1, q_2) = v_{\pi\pi\rho ex}(E', q_1, q_2) D_\rho(E', q_1, q_2), \quad (32)$$

where

$$D_\rho(E', q_1, q_2) = \frac{1}{t - m_\rho^2} \quad (33)$$

is the effective ρ t-channel propagator with 'renormalized' (physical) mass, $m_\rho = 770$ MeV, and 4-momentum transfer $t = (q_2 - q_1)^2$. The non-separability evades both an analytical solution of the scattering eq. (14) and a closed summation of the thermodynamic potential

eq. (21). Thus we are forced to evaluate the t-channel exchange contributions to $\Omega_{\pi\pi}(T)$ order by order. Fortunately there are two circumstances that will allow us to get a realistic estimate:

- the ρ t-channel exchange propagator, eq. (33), does not exhibit any poles in the kinematical region relevant for calculating the n -th order contribution to $\Omega_{\pi\pi}(T)$, thus ensuring the absence of divergencies order by order;
- as it will turn out from the numerical results in sect. 3.3 the series eq. (21) rapidly converges when summing the closed ladder sum (e.g. the third order contribution is typically 10% of the second order contribution).

When evaluating eq. (19) by using the expansion in eq. (15) with the pseudopotential (32) we encounter the same problem as was pointed out at the end of sect. 2.2.1, namely unrealistically large contributions from very high momenta. Therefore, as in the case of pole graphs, we replace the form factor entering the vertex functions in eq. (32) by

$$F(q, q)^2 \rightarrow F(k)F(p) . \quad (34)$$

By a slight readjustment of the form factor we made sure that the exact n -th order ρ exchange amplitude is reasonably well reproduced when using this separable approximation.

Another characteristic feature of the Jülich model is the occurrence of a scalar-isoscalar bound state in the coupled $K\bar{K}$ channel, just below the $K\bar{K}$ threshold. This bound state is generated by a strong attraction between kaon and antikaon, mediated by t-channel exchange of the vector mesons $\rho(770)$, $\omega(782)$ and $\phi(1020)$. It leads to the characteristic sharp rise in the $\pi\pi \rightarrow \pi\pi$ phase shifts δ^{00} in vicinity of the $K\bar{K}$ threshold and is interpreted as the $f_0(980)$. To incorporate this resonance-like feature of the $\pi\pi$ phase shifts in our calculation of $\Omega_{\pi\pi}(T)$ we proceed as follows: rather than summing the ladder diagrams involving the $K\bar{K}$ intermediate states and their direct interaction we simulate the $f_0(980)$ as a genuine resonance, *i.e.* we choose the resonance parameters such that

the full $\delta_{\pi\pi}^{00}$ phase shifts can be described without any coupling to the $K\bar{K}$ channel. The fully iterated $f_0(980)$ –polegraph contribution to $\Omega_{\pi\pi}(T)$ is then calculated as outlined in sect. 2.2.1 (eq. (28)).

Before ending this section we should point out that we have neglected any interference terms between the s–channel pole graphs ('bubble' sum) and the t–channel exchange graphs ('ladder' sum). The following two arguments make us believe that this is a reasonable approximation:

- the $\pi\pi$ interaction in the resonant channels (i.e. the $JI=11$ channel with the $\rho(770)$ –resonance and the $JI=20$ channel with the $f_2(1270)$ –resonance) is largely driven by polegraph contributions such that the additional incorporation of t–channel exchange processes is expected to have a quantitatively small effect; in the case of the ρ – and f_2 –channels the ρ t–channel exchange is attractive and leads to a rather small change of the resonance when evaluated with the combined ladder–/bubble–sum. Our results for the polegraph contribution, $\Omega'_{\pi\pi\alpha}(T)$, should therefore be considered as a lower estimate of the exact contribution; the situation is less clear for the (simulated) $f_0(980)$ in the $JI=00$ channel, but as it will turn out from the numerical results the f_0 –bubble sum gives a very small contribution by itself;
- as already mentioned in sect. 2.2.2 the ρ t–channel exchange contribution to $\Omega_{\pi\pi}(T)$ converges rapidly with the $(n+1)$ –th order being typically down by 10% from the n –th order.

We now turn to the evaluation of the single–(quasi–)pion part, $\Omega_{\pi}^Q(T)$, of the thermodynamic potential.

2.3 Quasiparticle Contributions: $\Omega_{\pi}^Q(T)$

In evaluating the contributions to $\Omega_{\pi}^Q(T)$ we shall also apply the QPA to the medium–modified single–pion spectrum, given by eq. (2). We essentially follow the steps outlined in ref. [24].

First we make use of the analytic properties of the one-pion propagator to transform the negative energy part of the ω -integration to positive values, namely

$$D_\pi(\omega_+, k) = D_\pi^*(\omega_-, k) . \quad (35)$$

Using the identity

$$Im[\ln(z)] = -Im[\ln(z^*)] \quad (36)$$

for any complex number z , and removing the infinite vacuum part (as discussed in sect. 2.1) results in

$$\Omega_\pi^Q(T) = -\frac{3}{2} \int \frac{d^3 k}{(2\pi)^3} \int_0^\infty \frac{d\omega}{\pi} 2f^\pi(\omega) Im\{\ln[-D_\pi^{-1}(\omega_+, k)] - D_\pi(\omega_+, k)\Sigma_\pi(\omega_+, k)\} . \quad (37)$$

The first term in the braces can be rewritten by using the identity

$$Im[\ln(-D_\pi^{-1}(\omega, k))] = \pi\Theta[ReD_\pi^{-1}(\omega, k)] - \arctan\left[\frac{-Im\Sigma_\pi(\omega, k)}{ReD_\pi^{-1}(\omega, k)}\right] . \quad (38)$$

Neglecting the imaginary part of Σ_π (which we will call scheme 'a') eq. (37) can be simplified as

$$\Omega_\pi^{Q,a}(T) = \frac{3}{2\pi^2} \int dk k^2 \left\{ T \ln(1 - e^{-e_k/T}) - \frac{1}{2e_k} f^\pi(e_k) Re\Sigma_\pi(e_k, k) \right\} . \quad (39)$$

The first term corresponds to the contribution of 'free' quasiparticles with modified dispersion relation $e_k = e(k)$, whereas the second term arises from an additional, dynamically generated, mean field. Their qualitative behavior is in line with the naive expectation that the pressure, $p = -\Omega$, is reduced for heavier particles but increases for a repulsive mean field and vice versa.

One can go one step further by including the imaginary part of the pion selfenergy in eq. (37) (which we will call scheme 'b'). Then $\Omega_\pi^Q(T)$ receives further contributions and reads

$$\begin{aligned} \Omega_\pi^{Q,b}(T) = & \frac{3}{2\pi^2} \int dk k^2 \left\{ T \ln(1 - e^{-e_k/T}) - \int_0^\infty \frac{d\omega}{\pi} f^\pi(\omega) \arctan\left[\frac{Im\Sigma_\pi(e_k, k)}{\omega^2 - \omega_k^2 - Re\Sigma_\pi(e_k, k)}\right] \right\} \\ & + \frac{3}{2\pi^2} \int dk k^2 \int_0^\infty \frac{d\omega}{\pi} f^\pi(\omega) \frac{Im\Sigma_\pi(e_k, k)(\omega^2 - \omega_k^2)}{(\omega^2 - e_k^2)^2 + (Im\Sigma_\pi(e_k, k))^2} . \end{aligned} \quad (40)$$

We shall consider both approximations, eqs. (39) and (40), in our numerical calculations discussed in the next chapter.

3 Thermodynamic State Variables and Numerical Results

3.1 Pressure, Entropy and Energy

Having the thermodynamic potential at hand, the state variables: pressure–density, $p(T)$, entropy–density, $s(T)$, and energy–density, $\epsilon(T)$, can be calculated by means of the standard thermodynamic relations at zero chemical potential:

$$p(T) = -\Omega(T) \quad (41)$$

$$s(T) = -\frac{\partial \Omega(T)}{\partial T} \quad (42)$$

$$\epsilon(T) = Ts(T) - p(T) . \quad (43)$$

As elaborated in refs. [24, 19] the partial derivative w.r.t. T in eq. (42) only acts on the explicit temperature dependence of the occupation factors due to the stationarity condition [24, 19]

$$\frac{\delta \Omega}{\delta \Sigma} = 0 . \quad (44)$$

Thus we obtain for the quasiparticle contributions to the entropy from eq. (39):

$$\begin{aligned} s_{\pi}^{Q,a}(T) = & \frac{3}{2\pi^2} \int dk k^2 \{ (1 + f^{\pi}(e_k)) \ln(1 + f^{\pi}(e_k)) - f^{\pi}(e_k) \ln(f^{\pi}(e_k)) \\ & - \frac{1}{2e_k} \frac{\partial f^{\pi}(e_k)}{\partial T} Re \Sigma_{\pi}(e_k, k) \} , \end{aligned} \quad (45)$$

or, when including a finite width for the pions, from eq. (40):

$$\begin{aligned} s_{\pi}^{Q,b}(T) = & \frac{3}{2\pi^2} \int dk k^2 \{ (1 + f^{\pi}(e_k)) \ln(1 + f^{\pi}(e_k)) - f^{\pi}(e_k) \ln(f^{\pi}(e_k)) \\ & - \int_0^{\infty} \frac{d\omega}{\pi} \frac{\partial f^{\pi}(\omega)}{\partial T} \arctan \left[\frac{Im \Sigma_{\pi}(e_k, k)}{\omega^2 - \omega_k^2 - Re \Sigma_{\pi}(e_k, k)} \right] \} \end{aligned}$$

$$+ \int_0^\infty \frac{d\omega}{\pi} \frac{\partial f^\pi(\omega)}{\partial T} \frac{Im\Sigma_\pi(e_k, k)(\omega^2 - \omega_k^2)}{(\omega^2 - \omega_k^2)^2 + (Im\Sigma_\pi(e_k, k))^2} \} , \quad (46)$$

which is consistent with the expressions quoted in ref. [24]. In our framework of meson-exchange interactions, the skeleton contributions to the entropy (denoted by $-\partial\Phi/\partial T$ in ref. [24]) arise in lowest order from eq. (12),

$$s_{\pi\pi}^{(1)}(T) = -\frac{3}{8} \int \frac{k dk}{(2\pi)^2 e_k} \int \frac{p dp}{(2\pi)^2 e_p} [I_A^{(1)} + I_B^{(1)}] \left[\frac{\partial f^\pi(e_k)}{\partial T} f^\pi(e_p) + f^\pi(e_k) \frac{\partial f^\pi(e_p)}{\partial T} \right] , \quad (47)$$

for the t-channel ρ exchange graphs from eq. (19),

$$\begin{aligned} s_{\pi\pi}^{(n)}(T) = & -\frac{3}{2} \frac{1}{4n} \int \frac{k^2 dk}{2\pi^2 2e_k} \int \frac{p^2 dp}{(2\pi)^2 2e_p} \int_{+1}^{-1} dx \int_0^\infty \frac{dE'}{\pi} Im M_{\pi\pi}^{(n)}(E', q, q) \times \\ & 2 \left[\frac{\partial F^\pi(E', k, p)}{\partial T} + \frac{\partial G^\pi(E', k, p)}{\partial T} \right] , \end{aligned} \quad (48)$$

and an analogous expression for the s-channel pole graphs from eq. (28) for $s_{\pi\pi\alpha}(T)$.

To check our results with respect to thermodynamic consistency, we will also consider an alternative way of evaluating the pressure density, namely

$$p_\pi(T) = \int_0^T dT' s_\pi(T') . \quad (49)$$

3.2 Selfconsistent Brueckner Scheme

As pointed out in sect. 2.1 the in-medium pion dispersion relation (or pion selfenergy) has to be determined selfconsistently from the Dyson eq. (8). In the QPA the pion selfenergy is given in terms of the in-medium and on-shell $\pi\pi$ forward scattering amplitude as [6]

$$\Sigma_\pi(e_k, k) = \frac{1}{k} \int_0^\infty \frac{dp}{(2\pi)^2} \frac{p}{2e_p} [f^\pi(e_p) - f^\pi(e_k + e_p)] \int_{E_{min}}^{E_{max}} dE_{cms} E_{cms} M_{\pi\pi}(E_{cms}) . \quad (50)$$

Here we have neglected the numerically very small contributions [22] from thermal excitations (as is usually done in the literature). The in-medium scattering amplitude, to be calculated from eq. (15), depends again on the pion selfenergy Σ_π through the in-medium two-pion propagator of the intermediate state:

$$G_{2\pi}(E, q) = \frac{1}{e_q} \frac{1 + 2f^\pi(e_q)}{E^2 - 4(\omega_q^2 + \Sigma_\pi(e_q, q))} . \quad (51)$$

Thus eqs. (8), (14), (50), (51) define a selfconsistency problem of Brueckner type which we solve (at fixed temperature) by numerical iteration as discussed in ref. [6].

The converged results for the pion selfenergy and the in-medium $M_{\pi\pi}$ -amplitude are then used to calculate the thermodynamic potential and state variables as described in sect. 2 and in sect. 3.1, respectively. According to scheme 'a' or 'b' (see sect. 2.3) we, respectively, either neglect or include $Im\Sigma_\pi$ when evaluating the two-pion propagator eq. (51).

3.3 Numerical Results and Discussion

For given value of the temperature we selfconsistently calculate the in-medium $\pi\pi$ amplitude as well as the pion selfenergy, which are then further used to evaluate the various contributions to the thermodynamic potential, namely

- (i) the lowest-order skeleton graphs, eq. (12);
- (ii) the resonance- $\pi\pi$ bubble skeleton graphs to all orders, eq. (28), for the resonances $\alpha = \rho(770), f_2(1270)$ and the simulated $f_0(980)$;
- (iii) the second- and third-order skeleton graphs for ρ t-channel exchange, eq. (19);
- (iv) the single-(quasi-)pion contributions given by eq. (39) or (40).

Let us first concentrate on scheme 'a' in which we neglect any imaginary part of the pion selfenergy. The full results for pressure-, entropy- and energy-density (full lines) are contrasted in fig. 1 with the results for free pions (dashed-dotted lines) and free ρ mesons (dotted lines). First we note that the quasiparticle contribution eq. (39) coincides at all temperatures within less than 1% with the EOS of free pions,

$$\Omega_\pi^{free}(T) = \frac{3T}{2\pi^2} \int dk k^2 \ln(1 - e^{-\omega_k/T}) . \quad (52)$$

The reason for that is an almost exact cancellation of the mean field contribution (second term in eq. (39)) and the kinematic modification caused by the replacement $\omega_k \rightarrow e_k$ in the exponential of the logarithm in the first term of eq. (39). But even the absolute

magnitudes of these medium-induced single-particle modifications do not exceed 3% at any temperature. These findings are at variance with the results of ref. [12], where a general *decrease* of the thermodynamic state variables compared to the free pion gas was found. This decrease is due to an increase of the in-medium pion mass dominantly leading to a suppression of the \ln -term in eq. (39). The increase of the pion mass stems from the net repulsion of the low-energy s-wave $\pi\pi$ interaction (Weinberg Lagrangian). In our analysis, however, it turns out that it is important to include both a higher energy range of the $\pi\pi$ interaction (essentially up to 1 GeV two-pion CMS energy) and higher partial waves. *E.g.* the resonant p-wave channel significantly contributes to $Re\Sigma_\pi(e_k, k)$, whereas there are large cancellations in both s- and d-wave between the attractive $I = 0-$ and the repulsive $I = 2-$ channels [11, 25].

Let us now come to the discussion of the skeleton diagrams. The effect of the first order graphs, eq. (12), is small: their combined contribution does not exceed 1% of $\Omega_\pi^{free}(T)$ in the considered temperature range. The most important role is played by the s-channel ρ -pole graphs, see *e.g.* table 1. It is remarkable that nearly half of the contribution to $p_{\pi\pi\rho}(T)$, $s_{\pi\pi\rho}(T)$ and $\epsilon_{\pi\pi\rho}(T)$ is due to negative energy contributions represented by the G^π -term in eq. (28). Without it the values for $p_{\pi\pi\rho}(T)$, $s_{\pi\pi\rho}(T)$ and $\epsilon_{\pi\pi\rho}(T)$ lie slightly below the free ρ -gas values $p_\rho^{free}(T)$, $s_\rho^{free}(T)$ and $\epsilon_\rho^{free}(T)$ (dashed-double-dotted lines in fig. 1). This is in agreement with the findings of ref. [11], *i.e.* that the $\pi\pi$ p-wave interaction effect resembles the presence of free ρ -mesons, the small suppression compared to the free ρ -gas values in our case being caused by the finite width of the ρ -resonance (which is even further broadened in medium) and the missing t-channel exchange diagrams. The latter, when implemented in the polegraph – $\pi\pi$ bubble sum, would lead to a slightly stronger renormalization of the bare ρ .

The effect of other $\pi\pi$ resonances is small: $p_{\pi\pi f_2}(T) = 3.8\% p_\pi^{free}$, $p_{\pi\pi f_0}(T) = 0.3\% p_\pi^{free}$ at $T=200$ MeV, and similarly for entropy- and energy-density. A somewhat larger contribution is generated by skeleton diagrams from second order ρ t-channel exchange, see *e.g.* table 2. The third order values are already one order of magnitude smaller.

The overall picture emerging for the temperature dependence of the thermodynamic state variables is quite similar for all three: we find an appreciable enhancement of the selfconsistently calculated pressure, entropy and energy for the interacting gas compared to free pions for temperatures $T \geq 100\text{MeV}$, which even exceeds the values for a free gas of pions and ρ -mesons. This excess can be traced back to negative energy contributions, naturally arising within our formalism, and low-energy t-channel exchange of virtual ρ -mesons between two pions. At very high temperatures ($T > 200\text{MeV}$) the thermal broadening of the $\pi\pi$ resonances, in particular the dominantly contributing $\rho(770)$, becomes so large that they no longer resemble the effect of an independent particle species (remember from the Beth–Uhlenbeck formalism that a sufficiently sharp two-particle resonance thermodynamically acts like an independent species corresponding to the quantum numbers of the resonance).

When including a finite width, $\text{Im}\Sigma_\pi$, for the quasi-pions (\equiv scheme 'b', as described in sect. 3.2.) we observe a slight overall enhancement of $p_\pi(T)$, $s_\pi(T)$ and $\epsilon_\pi(T)$ (dashed lines in fig. 1) compared to the results when neglecting $\text{Im}\Sigma_\pi$. The main source for this increase are the second order ρ t-channel skeleton graphs, the ρ pole skeleton graphs and the quasiparticle contributions eq. (40), compare table 3. In case of the skeleton diagrams this increase is simply due to the fact that $\text{Im}M_{\pi\pi}(E')$ acquires a nonzero imaginary part below the (in-medium) two-pion threshold all the way down to $E' = 0$. This leads to an additional contribution to the E' -integral in eqs. (19), (28), accounting for the almost entire difference in comparison to scheme 'a'.

We end this chapter by testing our numerical results with respect to thermodynamic consistency. For that we recalculate the total pressure-density by integrating the entropy-density according to eq. (49), which amounts to an implicit check of the stationarity condition, eq. (44). As can be seen from fig. 2 there is excellent agreement of the such calculated $p_\pi(T)$ with the 'direct' evaluation when neglecting the pion width (scheme 'a'). When including a finite $\text{Im}\Sigma_\pi$ (scheme 'b') the values for pressure-density obtained from eq. (49) are slightly suppressed as compared to the 'direct' calculation, causing a loss of

about half the enhancement over scheme 'a'.

4 Dropping Rho Meson Masses

In the calculations of the previous chapter no medium effects were considered in the interaction kernel of the $\pi\pi$ scattering equation. However, since our $\pi\pi$ model is based on explicit (vector) meson exchange, one may expect an impact on the pseudopotentials due to modifications in the propagator of the exchanged mesons when exposed to finite temperature. The most prominent example for such a modification is the dropping of the vector meson masses or 'Brown–Rho Scaling' [1, 3]. Adami and Brown suggested the temperature dependence of the ρ meson mass to be [2]

$$m_\rho(T) \approx m_\rho(0) \left(\frac{<\bar{q}q>_T}{<\bar{q}q>_0} \right)^{1/3}, \quad (53)$$

where $<\bar{q}q>_T$ denotes the quark condensate at finite temperature. The T dependence was taken as

$$<\bar{q}q>_T = <\bar{q}q>_0 \sqrt{1 - (T/T_c^\chi)^2}. \quad (54)$$

In ref. [25] such a decrease of the ρ mass was implemented in a selfconsistent pion gas calculation within the Jülich model as described in sect. 3.2.. Already well below T_c^χ a large accumulation of strength was found in the scalar–isoscalar channel of the $\pi\pi$ scattering amplitude close to the two–pion threshold. It is due to the strong enhancement of the attractive t–channel ρ exchange in this channel. However, it has been shown recently [26] that the implementation of chiral constraints into the $\pi\pi$ interaction is crucial to reliably calculate in–medium $\pi\pi$ correlations in the vicinity of the threshold. On the other hand, sufficiently above the two–pion threshold ($E_{cms} \geq 400\text{MeV}$ or so) chiral constraints rapidly cease to have significant impact on in–medium $\pi\pi$ amplitudes. This justifies the use of the non–chirally symmetric Jülich model in the previous chapter, where no dropping vector meson masses are taken into account and thus only minor threshold effects in the $\pi\pi$ amplitude are observed [6].

In this chapter we will employ a chirally improved version of the Jülich $\pi\pi$ interaction [31, 22]. It is supplemented with $\pi\pi$ contact interactions as required from the gauged nonlinear σ model [32]. To ensure the correct chiral limit for the s-wave scattering lengths a modified off-shell prescription for the pseudopotentials has been chosen when iterating the scattering eq. (14).

Due to the additional interaction terms in the Lagrangian of the chirally improved Jülich model there arise further contributions to the thermodynamic potential $\Omega_\pi(T)$. They are straightforwardly incorporated in the quasiparticle and in the lowest order contributions, $\Omega_\pi^Q(T)$ and $\Omega_{\pi\pi}^{(1)}(T)$, respectively. For $\Omega_{\pi\pi}^{(n)}(T)$ we take into account all contributions up to second order, namely from

- second-order ρ exchange as given by eq. (19) for $n=2$ with

$$\frac{1}{8} \text{Im}M_{\pi\pi}^{(2)} = \frac{1}{8} V_{\rho\text{ex}} \text{Im}G_{\pi\pi} V_{\rho\text{ex}} , \quad (55)$$

where we explicitly indicated the degeneracy factor $1/4n$;

- the second-order contact interactions also given by eq. (19) for $n=2$, but with the degeneracy factor $\frac{1}{8}$ replaced by $\frac{1}{4}$ due to the absence of exchange diagrams (compare the remarks following eq. (4)), *i.e.*

$$\frac{1}{4} \text{Im}M_{\pi\pi}^{(2)} = \frac{1}{4} V_{\text{cont}} \text{Im}G_{\pi\pi} V_{\text{cont}} ; \quad (56)$$

- the first-order ρ exchange plus first-order contact interaction; here the appropriate degeneracy factor is $\frac{1}{6}$:

$$\frac{1}{6} \text{Im}M_{\pi\pi}^{(2)} = \frac{1}{6} V_{\text{cont}} \text{Im}G_{\pi\pi} V_{\rho\text{ex}} . \quad (57)$$

Numerically it turns out that higher-order contributions in ρ exchange or contact interactions are again negligible.

When recalculating the EOS without any dropping of the ρ mass the results employing the chirally improved Jülich model differ by around 5% from those presented in sect. 3.3,

confirming the notion that chiral symmetry has little impact on the $\pi\pi$ interaction as long as strong threshold effects are absent.

Let us now turn to the scenario with 'Brown–Rho Scaling' included. For simplicity we will neglect the coupling to the $K\bar{K}$ channel, which was shown to have a very small effect in the previous chapter. Relevant for our model are the decrease of the (physical) ρ mass (eq. (53)) and the corresponding reduction of the pion decay constant,

$$\frac{f_\pi(T)}{f_\pi(0)} = \frac{m_\rho(T)}{m_\rho(0)} . \quad (58)$$

The latter enters the $\pi\pi$ contact interactions, whereas the physical mass m_ρ is used in the t–channel ρ exchange propagator, eq. (33). For given temperature the bare ρ mass $m_\rho^{(0)}$ used in the s–channel ρ pole propagator, eq. (23), is adjusted such that the fully renormalized $M_{\pi\pi}^{11}$ –amplitude in free space acquires its maximum (i.e. ρ resonance peak) at the corresponding value of $m_\rho(T)$ from eqs. (53), (54). For fixed $m_\rho(T)$, $f_\pi(T)$ and $m_\rho^{(0)}(T)$ we then perform selfconsistent Brueckner calculations for Σ_π and $M_{\pi\pi}$ at several T –values along exactly the same lines as described in sect. 3.2.

The resulting EOS for the hot interacting pion gas is displayed in fig. 3, where we have chosen the critical temperature of chiral symmetry restoration to be $T_c^\chi=170$ MeV. For $T \geq 100$ MeV we observe a strong increase of the thermodynamic state variables as compared to the calculations without inclusion of the Brown–Rho Scaling. Most of the effect is of simple kinematic origin, as can be seen by comparison to the free π – ρ gas including the decrease of m_ρ . However, for temperatures below $T \approx 150$ MeV the $\pi\pi$ interactions still generate an enhancement over the free π – ρ case of up to 15%, which is quite similar to what we found in the pure Brueckner calculations. Just below T_c^χ the free π – ρ gas values for $p_\pi(T)$, $s_\pi(T)$ and $\epsilon_\pi(T)$ are close to the ones of the interacting pion gas. This is due to the fact that the ρ polegraph starts acquiring appreciable renormalization contributions especially from the strongly attractive t–channel exchange of a ρ meson of mass $m_\rho(T)$. However, in our approximation scheme for $\Omega_{\pi\pi}(T)$, this kind of contributions is not accounted for (compare sect. 2.2.1), even though they are certainly not negligible anymore in the vicinity of T_c^χ .

5 Summary and Conclusions

Based on the finite-temperature Greens-function formalism we have presented an analysis of the equation of state of a hot interacting gas of pions at zero chemical potential.

Starting from a realistic $\pi\pi$ meson-exchange model capable of describing the vacuum scattering data over a broad range of energies we have calculated the in-medium $\pi\pi$ scattering amplitude and the single-pion selfenergy. The resulting selfconsistency problem has been solved by numerical iteration within the quasiparticle approximation (Brueckner scheme) [6].

We then proceeded to evaluate the thermodynamic potential $\Omega_\pi(T)$:

- the single-pion selfenergy was used for calculating the quasiparticle contribution $\Omega_\pi^Q(T)$; the latter turned out to be very close to the values for free pions due to a cancellation between the mean field term and the free quasi-pion term (only when including a finite width for the pions a $\approx 5\%$ enhancement was found);
- for the interaction part of the thermodynamic potential, $\Omega_{\pi\pi}(T)$, we have taken into account the $f_0(980)-$, $\rho(770)-$ and $f_2(1270)-$ s-channel pole graphs to all orders as well as the ρ t-channel exchange up to third order; higher orders as well as interference terms between s- and t-channel graphs have been estimated to be small and were neglected; the main contribution stems from the ρ pole graphs, their magnitude being comparable to what one expects from an admixture of free ρ mesons.

Special attention has been paid to constraints from thermodynamic consistency, and it was shown that our results satisfactorily fulfill these constraints.

In total we have found a 10–15% enhancement of $\Omega_\pi(T)$ compared to a free gas of π and ρ mesons in the temperature range $100 \text{ MeV} \leq T \leq 150 \text{ MeV}$. Pressure-, entropy- and energy-density, which were extracted from $\Omega_\pi(T)$ by means of standard thermodynamic relations, show a very similar behavior. This is in qualitative agreement with the results of Welke et al. [11], who employed empirical vacuum s- and p-wave $\pi\pi$ phase shifts

within a relativistic virial expansion. Our results are, however, at qualitative variance with the findings of Bunatian and Kämpfer [12], who also used the finite temperature Greens–function approach but employed the Weinberg Lagrangian. The latter is known to account only for the low–energy s–wave $\pi\pi$ interaction, resulting in a net repulsion when performing the isospin weighted sum for the near–threshold $\pi\pi$ amplitude. As a consequence, their thermodynamic state variables show an overall *decrease* with temperature as compared to the free pion gas.

Our conclusion from this is that the higher energy range (up to CMS energies close to 1 GeV) as well as higher partial waves (especially the resonant p–wave) in the $\pi\pi$ interaction are important for a reliable description of thermodynamic properties of an interacting gas of pions.

We furthermore investigated the impact of a dropping ρ mass according to 'Brown–Rho Scaling'. Using a chirally improved Jülich model including contact interactions, arising from the gauged Weinberg Lagrangian, we find a similar behavior as before: even though the thermodynamic state variables of the interacting pion gas now exhibit a considerable increase near T_c^χ , the enhancement over the free π – ρ gas values (dropping ρ mass included) is not more than 10–20%. Very close to the critical temperature, where the ρ mass rapidly drops to zero, the interacting pion gas values are close to the ones of the free π – ρ gas. This feature, however, is due to the breakdown of our approximations; in particular, interference terms between ρ s– and t–channel graphs become far from negligible.

the strong gauge 'data'. ('external') however,

Acknowledgement

We thank G.G. Bunatian, D. Blaschke and J. W. Durso for useful discussions. One of us (R.R.) acknowledges financial support by Deutscher Akademischer Austauschdienst

(DAAD) under program HSPII/AUFE. This work was supported in part by a grant from the National Science Foundation, NSF-PHY-94-21309.

References

- [1] G. E. Brown and M. Rho, Phys. Rev. Lett. **66** (1991) 2720.
- [2] C. Adami and G. E. Brown, Phys. Rep. **234** (1993) 1. **84** (1994) 281.
- [3] T. Hatsuda, Nucl. Phys. **A544** (1992) 27c;
T. Hatsuda, Y. Koike and S.H. Lee, Nucl. Phys. **B394** (1993) 221; Phys. Rev. **D47** (1993) 1225.
- [4] E.V. Shuryak, Nucl. Phys. **A533** (1991) 761.
- [5] A. Schenk, Nucl. Phys. **B363** (1991) 97.
- [6] R. Rapp and J. Wambach, Phys. Lett **B315** (1993) 220.
- [7] G. Chanfray and D. Davesne, Zeit. Phys. **A349** (1994) 65.
- [8] J. L. Goity and H. Leutwyler, Phys. Lett. **B228** (1989) 517.
- [9] Z. Aouissat, G. Chanfray, P. Schuck and G. Welke, Zeit. Phys. **A340** (1991) 347.
- [10] H.W. Barz, G.F. Bertsch, P. Danielewicz and H. Schulz, Phys. Lett. **B275** (1992) 19.
- [11] G. M. Welke, R. Venugopalan and M. Prakash, Phys. Lett. **B245** (1990) 137;
R. Venugopalan and M. Prakash, Nucl. Phys. **A546** (1992) 718.
- [12] G.G. Bunatian and B. Kämpfer, preprint FZR 93-28.
- [13] S. Gavin, Nucl. Phys. **B351** (1991) 561.
- [14] H. Von Gersdorff, M. Kataja, P. V. Ruuskanen and M. Mc Lerran, Phys. Rev. **D34** (1986) 794.
- [15] G.M. Welke and G.F. Bertsch, Phys. Rev. **C45** (1992) 1403;
H.W. Barz, P. Danielewicz, H. Schulz and G.M. Welke, Phys. Lett. **B287** (1992) 40.

- [16] G. E. Beth and E. Uhlenbeck, *Physica* **3** (1936) 729; **4** (1937) 915.
- [17] S. Weinberg, *Phys. Rev. Lett.* **18** (1967) 188.
- [18] D. Lohse, J.W. Durso, K. Holinde and J. Speth, *Phys. Lett.* **B234** (1989) 235;
Nucl. Phys. **A516** (1990) 513;
B. C. Pearce, K. Holinde and J. Speth, *Nucl. Phys.* **A541** (1992) 663.
- [19] A. A. Abrikosov, L. P. Gorkov and I. E. Dzyalosinski, '*Methods of Quantum Field Theory in Statistical Physics*', Prentice Hall, Englewood Cliffs, N. J. 1963.
- [20] G. G. Bunatian and J. Wambach, *Phys. Lett.* **B336** (1994) 290.
- [21] R. Blankenbecler and R. Sugar, *Phys. Rev.* **142** (1966) 1051.
- [22] R. Rapp and J. Wambach, *Phys. Lett.* **B351** (1995) 50.
- [23] J. A. Johnstone and T.-S. H. Lee, *Phys. Rev.* **C34** (1986) 243.
- [24] G. M. Carneiro and C. J. Pethick, *Phys. Rev.* **B11** (1975) 1106.
- [25] R. Rapp, Diplomarbeit, Bonn 1993, unpublished.
- [26] Z. Aouissat, R. Rapp, G. Chanfray, P. Schuck and J. Wambach, *Nucl. Phys.* **A581** (1995) 471.
- [27] L.P. Kadanoff and G.A. Baym, '*Quantum Statistical Mechanics*', Benjamin, New York 1962.
- [28] L.D. Fetter and J.D. Walecka, '*Quantum Theory of Many Particle Systems*', Mc Graw Hill, New York 1971.
- [29] M. Schmidt, G. Röpke and H. Schulz, *Ann. Phys.* **202** (1990) 57.
- [30] R. Rapp and J. Wambach, *Nucl. Phys.* **A573** (1994) 626.
- [31] R. Rapp, J. W. Durso and J. Wambach, *Nucl. Phys. A*, in press.

[32] S. Weinberg, Phys. Rev. **166** (1968) 1568.

Tables

T [MeV]	$p_{\pi\pi\rho}/p_{\pi}^{free}$	$s_{\pi\pi\rho}/s_{\pi}^{free}$	$\epsilon_{\pi\pi\rho}/\epsilon_{\pi}^{free}$
150	26%	41%	45%
200	43%	56%	60%

Table 1: Contributions from the ρ pole graph skeleton diagrams to the thermodynamic state variables in an interacting hot pion gas within the Brueckner calculations neglecting any width of the pions.

T [MeV]	$p_{\pi\pi\rho ex}^{(2)}/p_{\pi}^{free}$	$s_{\pi\pi\rho ex}^{(2)}/s_{\pi}^{free}$	$\epsilon_{\pi\pi\rho ex}^{(2)}/\epsilon_{\pi}^{free}$
150	7.0%	8.5%	8.9%
200	9.8%	11.2%	11.7%

Table 2: Contributions from the 2.order ρ t-channel exchange skeleton diagrams to the thermodynamic state variables of an interacting hot pion gas within the Brueckner calculations, neglecting any width of the pions.

	$p_{\pi\pi\rho ex}^{(2)}/p_{\pi}^{free}$	$p_{\pi\pi\rho}/p_{\pi}^{free}$	p_{π}^Q/p_{π}^{free}	$p_{\pi}^{tot}/p_{\pi}^{free}$
$Im\Sigma_{\pi} \equiv 0$	9.8%	43%	99.8%	158.4%
$Im\Sigma_{\pi} < 0$	13.3%	46.6%	107.6%	173.7%

Table 3: Various contributions to the pressure density of an interacting hot pion gas at $T = 200$ MeV within the Brueckner calculations when neglecting (upper line) and including (lower line) a finite pion width.

Figure Captions

Fig. 1: Thermodynamic state variables (scaled by temperature to dimensionless units) of an interacting hot pion gas within the Brueckner scheme with no medium modifications applied to the two-body interaction potentials;
 upper panel: pressure-density;
 middle panel: entropy-density;
 lower panel: energy-density;
 full lines: interacting pion gas when neglecting the pion width; dashed lines: interacting pion gas with inclusion of a finite pion width; dotted lines: free ρ gas;
 dashed-dotted lines: free pion gas; dashed-double-dotted lines: free $\pi-\rho$ gas.

Fig. 2: Comparison of two different ways of calculating the pressure-density of an interacting pion gas within the Brueckner scheme; the full line ($Im\Sigma_\pi$ neglected) and the dashed-dotted line ($Im\Sigma_\pi$ included) correspond to the 'direct' calculations (the sum of eqs. (12), (19), (28) and (39)/(40)), whereas the dashed line ($Im\Sigma_\pi$ neglected) and the dotted line ($Im\Sigma_\pi$ included) are obtained from integrating the entropy-density according to eq. (49).

Fig. 3: Thermodynamic state variables (scaled by temperature to dimensionless units) of an interacting hot pion gas within the Brueckner scheme plus additional medium modifications of the two-body pseudopotentials in form of dropping $m_\rho(T)$ and $f_\pi(T)$; here, a chirally improved version of the Jülich $\pi\pi$ interaction has been employed;
 upper panel: pressure-density;
 middle panel: entropy-density;
 lower panel: energy-density;
 line identification as in fig. 1.

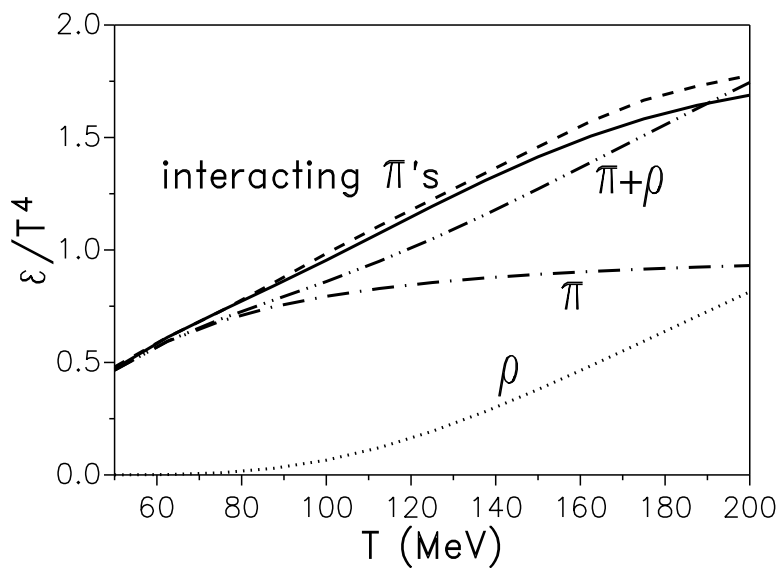
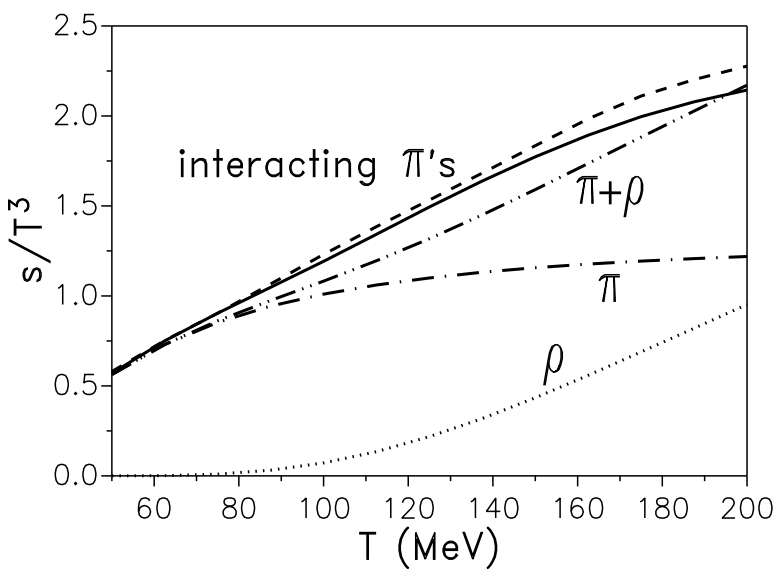
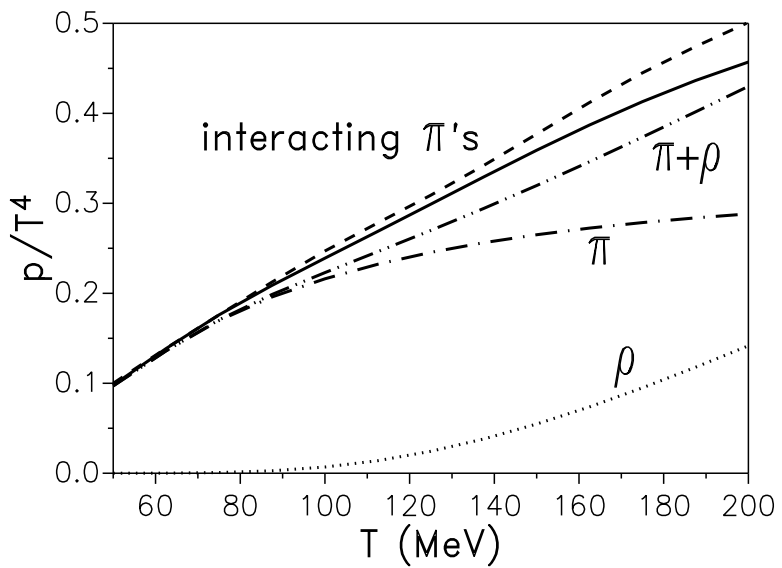
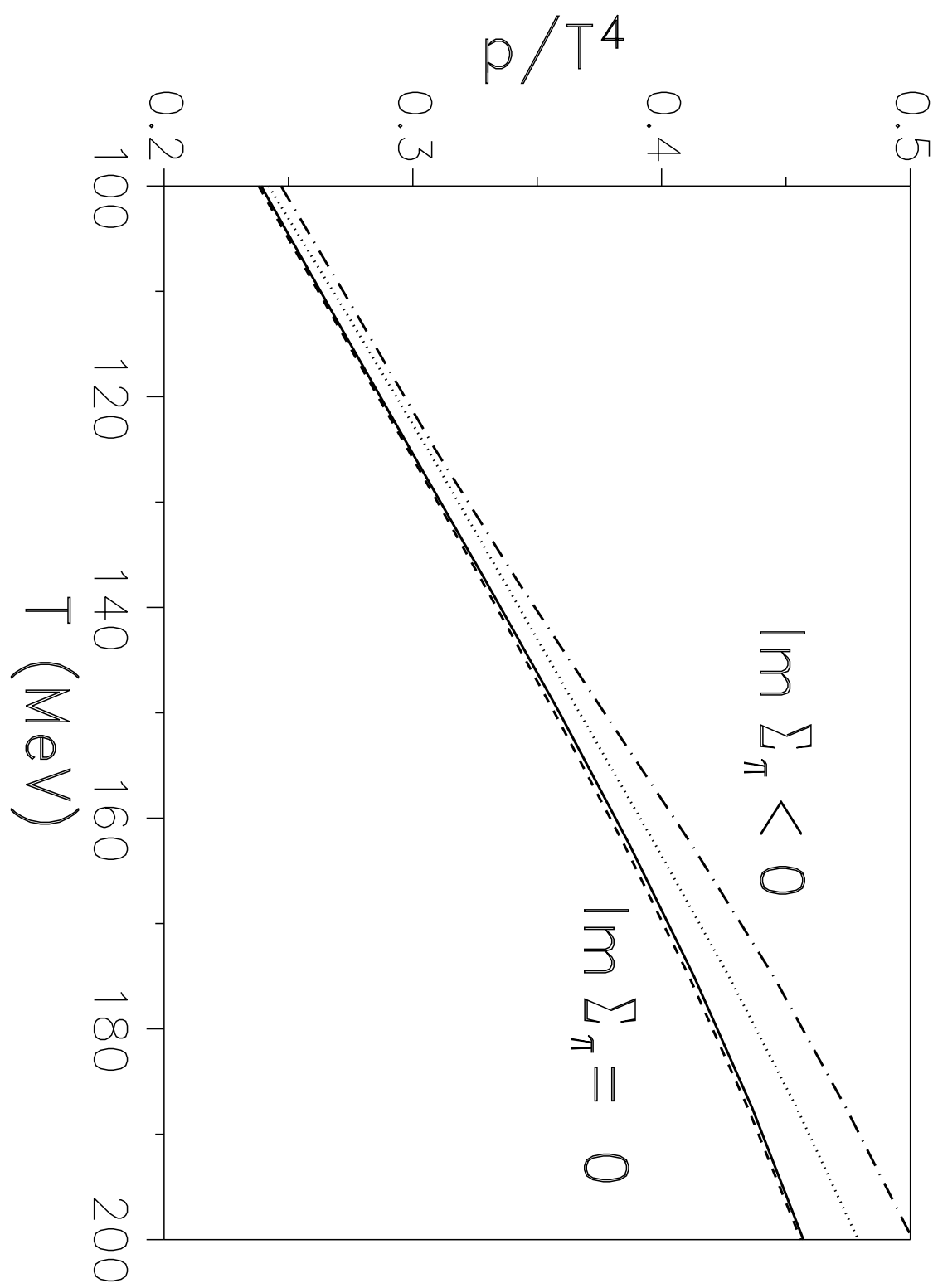


Fig. 1

Fig. 2



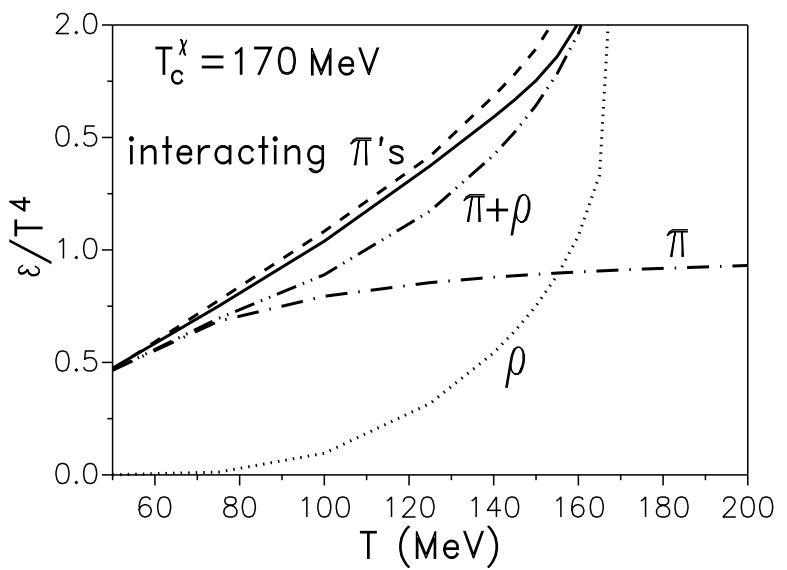
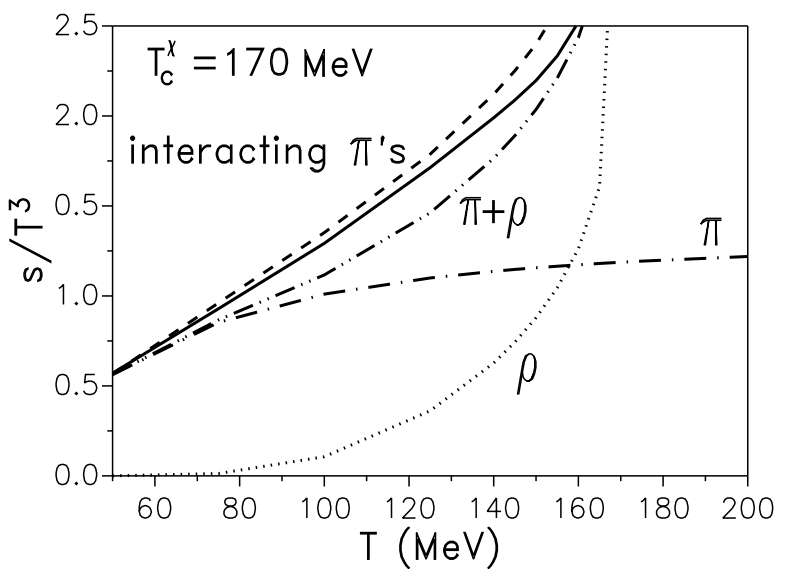
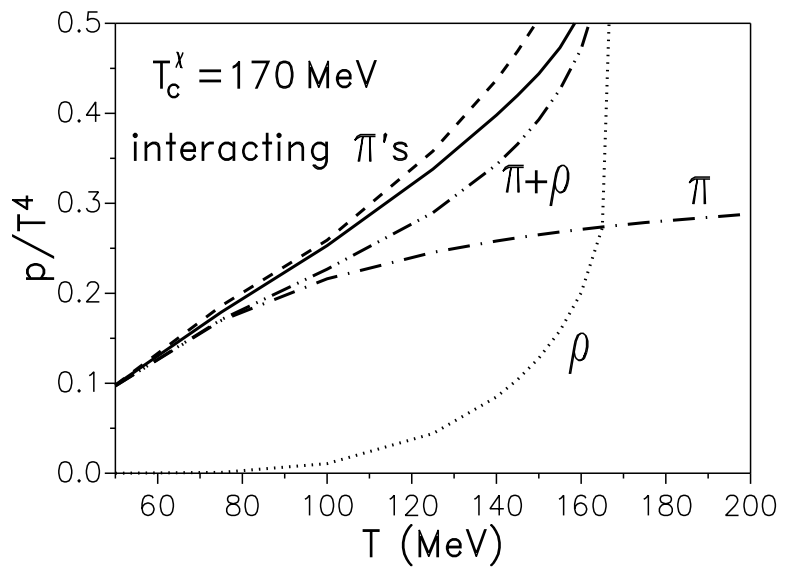


Fig. 3